

# Dependence of Radial Structure of Collisionless Trapped Ion Mode on Pressure and $q$ Profiles

LI Jiquan<sup>1,2\*</sup>, KISHIMOTO Yasuaki<sup>1</sup>, TUDA Takashi<sup>1</sup> and ZHANG Jinhua<sup>2</sup>

<sup>1</sup> Naka Fusion Research Establishment, JAERI, Naka, Ibaraki, 311-0193, Japan

<sup>2</sup> Southwestern Institute of Physics, P.O.Box 432, Chengdu, Sichuan 610041, P.R.China

(Received: 5 December 2000 / Accepted: 18 August 2001)

## Abstract

The radial eigen equation of the collisionless trapped ion mode (CTIM) is re-derived by directly retaining the effect of finite banana orbit width. Local and non-local stability analyses and the dependence of radial mode structure on both pressure and  $q$  profiles are presented. It is found that the radial structure of CTIM is dominated by the competition between the non-adiabatic trapped ion and passing ion dynamics. The discussion related to the results from recent toroidal particle simulations and the two-dimensional eigenmode code is given.

## Keywords:

collisionless trapped ion mode (CTIM), stability analysis, radial mode structure, pressure profile,  $q$  profile

## 1. Introduction

Recent toroidal particle simulations on the ion temperature gradient mode [ITG or  $\eta_i (= d \ln T_i / d \ln n)$ ] with weak or reversed magnetic shear have shown some interesting mode structures [1-3]. One is the repetition of formation and destruction of a discontinuous global mode near the minimum- $q$  surface in reversed shear plasmas, which has been testified to work efficiently as an internal transport barrier (ITB) [1,2]. The candidates for its formation may include the non-resonant mode [1] and the sheared slab mode with separate structures near the minimum- $q$  surface [4]. Its destruction seems to exhibit some characters of the collisionless trapped ion mode (CTIM). Another is a typically global ballooning structure in the case with a linear  $q$  profile [3]. However, it is observed that the radial mode width shrinks as the magnetic shear  $\hat{s}$  tends to be weak. This seems to be not consistent with the standard ballooning mode analysis, which shows the global mode width  $\Delta r \propto \hat{s}^{-1/2}$  with moderate or strong shear. Further Fourier

mode decomposition shows that the mode resonant surface of each poloidal harmonic, which the eigenfunction is localized in its vicinity, deviates from the rational surface with  $k_{\parallel} = 0$  and draws toward the surface with maximum- $\nabla p$ . This also recalls CTIM which is insensitive to the magnetic shear and is excited near the maximum- $\nabla p$  surface [5]. Motivated by these considerations, the radial structure of CTIM and the parametric dependence are re-investigated to further understand the global mode structure and the relevant anomalous ion transport observed in the toroidal particle simulations.

## 2. Radial Eigen Mode Equation of CTIM

In tokamak plasmas, the trapped ion mode is a typical low-frequency and long wavelength collective mode with  $\hat{\omega}_{Di} < \omega < \omega_{bi}$  [6]. Here  $\hat{\omega}_{Di} = 2k_{\theta} c T_i / e B_0 R$  and  $\omega_{bi} = \sqrt{2} \epsilon v_{ti} / q R$  with  $\epsilon = a/R$ . The electrostatic CTIM is described by the quasineutrality condition and

\*Corresponding author's e-mail: jqli@PTL01.naka.jaeri.go.jp

the drift kinetic equation for the non-adiabatic part,  $h_j$ , of perturbed distribution function due to the banana orbit width  $\rho_{bi}(=q\rho_i/\sqrt{\epsilon})$  being larger than ion Larmor radius  $\rho_i$ . Usually,  $h_j$  for trapped ions can be solved step by step through ordering a small quantity  $\hat{\epsilon} = \omega/\omega_{bi}$ . However, the radial excursion of trapped ions, namely the finite banana width effect, is retained here in the lowest order equation, i.e.,

$$\frac{v_{\parallel}(\theta)}{qR} \frac{\partial}{\partial \theta} h_{j0}(r, \theta) + \vec{v}_{Dr} \cdot \nabla_r h_{j0}(r, \theta) = 0, \quad (1)$$

with  $v_{Dr} = -(\sin\theta/R\Omega_{ci})(v_{\perp}^2/2 + v_{\parallel}^2)$ . Here  $\Omega_{ci} = eB_0/m_i c$ . Using the relation  $\partial v_{\parallel}(\theta)/\partial \theta \approx -(\mu B_0 e/m_i) \sin\theta/v_{\parallel}(\theta)$  with  $\mu = v_{\perp}^2/2B_0$  for trapped particles [7], it yields

$$h_{j0}(r, \theta) = h_{j0}(r) \exp\left[\frac{ik_r 2q v_{\parallel}(\theta)}{\epsilon \Omega_{ci}} \left(\frac{1}{2} + \frac{v_{\parallel}^2}{v_{\perp}^2}\right)\right], \quad (2)$$

after employing the transformation  $\nabla_r \rightarrow -ik_r$ . Note that the exponential term describes in fact the effect of the finite banana orbit width due to  $\rho_{bi} \propto v_{\parallel}/\epsilon \Omega_{ci}$ . It can be expanded in small argument. The similar zero order solution has also been given in Ref.8. Guided by the fully 2-Dimensional (poloidal and radial) eigenmode analysis for CTIM [5,9] which shows the full 2-D results are in qualitative agreement with those from the 1-D radial studies for weak magnetic shear case,  $h_{j0}(r)$  can be obtained from the next order equation under using the bounce-averaging approximation as usual [10]. Employing the usual expressions for the trapped electron and passing ion responses [6] and using the inverse transformation  $-ik_r \rightarrow d/dr$ , the radial eigen equation of CTIM can be obtained from the quasi-neutrality condition, i.e.,

$$\rho_{bi}^2 A_r \frac{d^2}{dr^2} \phi + \left[ -\frac{1+\tau}{2\tau\sqrt{2\epsilon}} + \delta_{iT} + \frac{\delta_{eT}}{\tau} + \frac{\delta_{iC}}{2\sqrt{2\epsilon}} \right] \phi = 0, \quad (4)$$

with

$$A_r = \int_T \frac{d^3 v \left( 4 \langle v_{\parallel}^2(\theta) \rangle / \epsilon \right) \left( \omega - \langle \omega_{*Ti} \rangle \right) F_M}{\omega - \left( k_{\theta} \langle \cos\theta \rangle / R \Omega_{ci} \right) \left( v_{\perp}^2/2 + v_{\parallel}^2 \right)} \left( \frac{1}{2} + \frac{v_{\parallel}^2}{v_{\perp}^2} \right)^2,$$

$$\delta_{iT} = \int_T \frac{d^3 v \left( \omega - \langle \omega_{*Ti} \rangle \right) F_M}{\omega - \left( k_{\theta} \langle \cos\theta \rangle / R \Omega_{ci} \right) \left( v_{\perp}^2/2 + v_{\parallel}^2 \right)}.$$

Here  $\tau = T_e/T_i$ ,  $\omega_{*Tj} = (k_{\theta} c T_j / q B_0 L_n) [1 + \eta_j (v^2/v_{Tj}^2 - 3/2)]$  with  $L_n = (d \ln n/dr)^{-1}$ ,  $F_M$  is Maxwellian distribution function, and  $\langle \dots \rangle$  indicates usual bounce-averaging. The passing ion response  $\delta_{iC}$  is the same as that in Ref.6, which includes the dependence on the magnetic shear, i.e.,  $q$  profile. Eq.(4) is different from its usual counterpart [9] obtained by employing the approximate expansion  $\langle \phi(r, \theta) \rangle = \phi(r_0) + \rho_{bi}^2 d^2 \phi(r_0)/dr_0^2$ , it includes the effect of all different banana orbit width on the radial structure.

### 3. Stability Analysis of CTIM

Local analysis: generally, the local approximation (ignoring the radial derivative) is advisable to predict the existence of the instability. Fig.1(a) shows that there exist two pairs of unstable branches of local pure CTIM (with  $\delta_{iC} = 0$ ) for steeper pressure gradient, i.e., smaller  $\epsilon_p [= (d \ln p/dr)^{-1}/R]$ . Note that all branches become aperiodic (real frequencies are zero) in region II, and branches labeled by 2 and 4 degenerate into one. It is identified that the branch labeled by 3 corresponds to the residual trapped ion mode [11]. It is further shown that this branch can remain in plasmas with  $L_n \rightarrow \infty$  and  $\delta_{eT} = 0$ , and it is hardly stabilized by non-adiabatic passing ion dynamics.

Non-local analysis: for simplicity, assuming a parabolic-type pressure gradient model  $\epsilon_p = \epsilon_{p0}(1 + x^2/L_p^2)$  near the maximum- $\nabla p$  surface  $r = r_0$  with  $x = (r - r_0)/\rho_i$ , the thick dashed and solid curves in Fig.1(b) illustrate the typical non-local growth rates and real frequencies versus  $\epsilon_{p0}$  (lower horizontal axis) corresponding to the local branches. It can verify the local results, even including the degeneration of branches labeled by 2 and 4. For a more realistic model of pressure profile  $n_e \sim T_i = T_e = 1 + 6.5/[1 + e^{D(\rho - 0.5)}]$  with  $\rho = r/a$  and constant  $D$  for adjusting the pressure profile, typically for profiles of JT-60U, the local results are further testified by the thin curves corresponding to the thick ones as shown in Fig.1(b).

### 4. Radial Structure of CTIM

For pure CTIM, the eigen mode possesses a wider slab-like radial structure near the maximum- $\nabla p$  surface and it is almost independent of the magnetic shear, i.e.,  $q$  profile. However, when the non-adiabatic passing ion response is included, the Landau damping near the rational surface can not only play a stabilizing role to CTIM, but also change the mode structure. Assuming a nearly flat  $q$  profile such as  $q = 0.9 a e^{\sigma \rho}$  similar to that in the toroidal particle simulations, and employing the

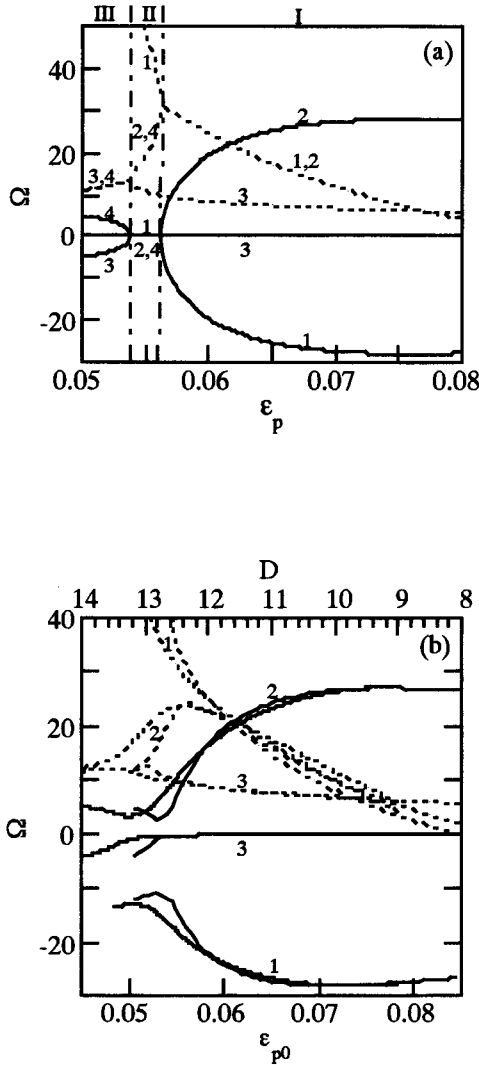


Fig. 1 Normalized real frequencies (solid) and growth rates (dashed) of CTIM by  $\hat{\omega}_{\text{be}}$  versus pressure gradient parameter for local (a) and non-local (b) cases.  $\tau \approx 1$ ,  $\eta_i = \eta_e \approx 1$ ,  $\epsilon = 0.325$ ,  $q = 1$ ,  $L_p = 200\rho_i$ . Note that two sets of curves from two pressure profile models are included in case (b) against the local case (a), the thick curves correspond to lower horizontal axis and the thin curves are to the upper one.

realistic model of pressure profile used in Fig.1(b) with different constant  $D$ , Fig.2 displays the dependence of the resonant surfaces of CTIM on both pressure and  $q$  profiles. For a flatter pressure profile (smaller  $D$  case), the trapped ion dynamics is relatively weaker, the resonant surface of each  $m$ -harmonic is almost located near the corresponding rational surface. The mode has usual character of the slab  $\eta_i$  mode except for the wider

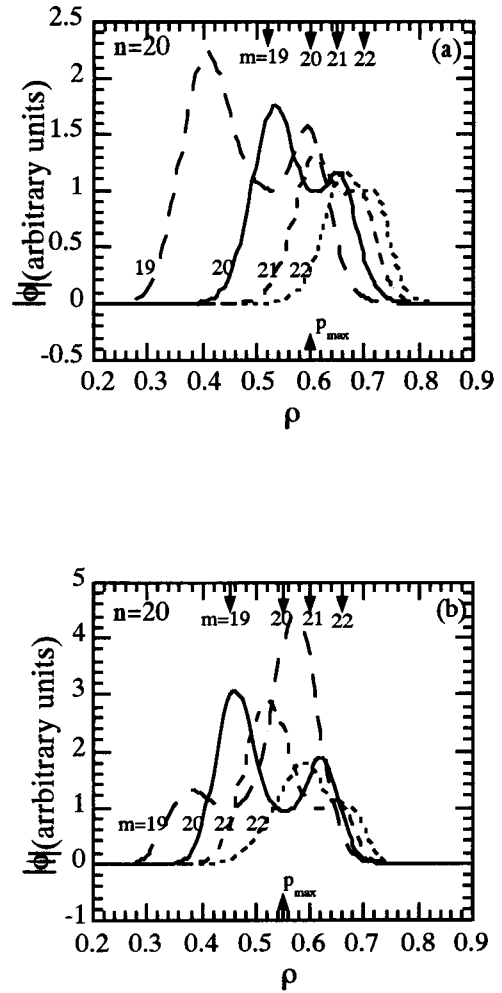


Fig. 2 Mode structure of different  $m$ -harmonics for typical parameters of JT-60U.  $\tau \approx 1$ ,  $\epsilon = 0.325$ ,  $R \approx 300$  cm,  $a \approx 100$  cm,  $\rho_i \approx 0.3$  cm. (a):  $D = 10$ ,  $\alpha = 0.00095$ ,  $\sigma = 7.7$ ; (b):  $D = 20$ ,  $\alpha = 0.003$ ,  $\sigma = 6.5$ .

radial structure. In addition, it can be seen the high- $m$  harmonics possess narrower radial width due to the localization of magnetic shear. However, as the pressure gradient becomes steeper, the trapped ion dynamics tends to be stronger. The resonant surface of each  $m$ -harmonic deviates from the corresponding rational surface and draws toward the maximum- $-\nabla p$  surface, except for the harmonic  $m = 20$  due to its rational surface coinciding with the maximum- $-\nabla p$  surface. This shows that the radial structure of CTIM is dominated by the competition between the non-adiabatic trapped ion and passing ion dynamics. The former is governed by the pressure profile and magnetic trapping, the latter strongly depends on  $q$  profile. This picture can be

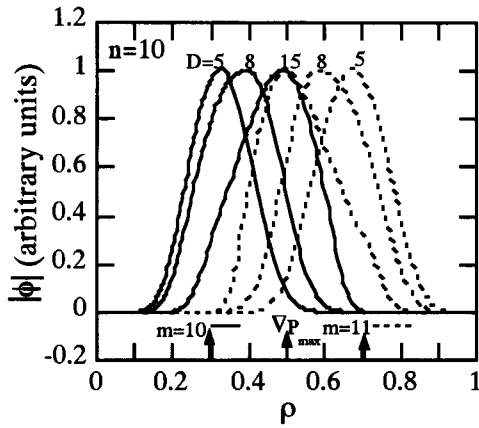


Fig. 3 Dependence of the resonant surfaces of  $m$ -harmonics on the pressure profile for the case with a linear  $q$  profile and without trapped electron response. The solid curves correspond to  $m = 10$ , the dashed ones to  $m = 11$ .  $\tau \approx 1$ ,  $\varepsilon = 0.325$ ,  $R \approx 300$  cm,  $a \approx 100$  cm,  $\rho_i \approx 0.3$  cm,  $L_n \rightarrow \infty$ .

further illustrated clearly by Fig.3, where only two rational surfaces are included due to the flatly linear  $q$  profile  $q = 0.925 + 0.25\rho$  similar to that in the simulation [3].

## 5. Summary and Discussion

In this work, a radial eigen equation of CTIM including the effect of all different banana orbit widths is re-derived. Local and non-local stability analyses for a steeper pressure profile show that the more important branch of CTIM is the residual trapped ion mode. Its radial structure is dominated by the competition between the non-adiabatic trapped ion and passing ion dynamics, namely depends on both pressure and  $q$  profiles.

This one-dimensional picture for the radial structure of CTIM is helpful to understand the global mode structures observed in the toroidal particle simulations. In a plasma with negative shear [1,2], after the formation of discontinuous global structure near the minimum- $q$  surface, the heat is isolated inside, the temperature profile tends to be steeper, CTIM may be excited and the discontinuity disappears. Soon afterwards, the heat is ejected through the global mode and the temperature relaxes, CTIM may become marginally stabilizing, finally the discontinuity recovers. For a plasma with linear  $q$ -profile [3], as  $q$  profile

becomes flatter, the trapped ion dynamics relatively tends to be stronger than the passing ion dynamics. Hence, the global structure may be dominated by the CTIM, and the global mode width could shrink due to all  $m$ -harmonics drawing toward the maximum- $\nabla p$  surface. Furthermore, this one-dimensional picture can also explain the mode structure from 2-D eigenmode code as shown in Fig.1 of Ref.5. For the given equilibrium pressure and  $q$  profiles, the magnetic trapping effect is stronger in the unfavorable curvature region ( $\theta \approx 0$ ), the radial locations of all  $m$ -harmonics are dominated by the trapped ion dynamics. All  $m$ -harmonics draw toward the maximum- $\nabla p$  surface to form an extended radial structure. On the other hand, near  $\theta \approx \pi$  surface, the magnetic trapping is almost marginal and the passing ion dynamic is dominant. Landau damping leads to the localization of all  $m$ -harmonics near the corresponding rational surfaces which is almost independent of the variation of the equilibrium pressure gradient.

## Acknowledgments

One of authors (Li) would like to thank Dr. G. Rewoldt and Prof. W.X. Qu for their discussions. This work was supported by Science and Technology Agency of Japan. It was also supported in part by National Natural Science Foundation of China under grant No.19705004 and National Nuclear Science Foundation of China.

## References

- [1] Y. Kishimoto *et al.*, Plasma Phys. Control. Fusion **40**, A663 (1998).
- [2] Y. Kishimoto *et al.*, Nucl. Fusion **40**, 667 (2000).
- [3] Y. Kishimoto *et al.*, in Fusion Energy 1996 (IAEA, Montreal) **2**, 581 (1997).
- [4] Jiquan Li *et al.*, Plasma Phys. Control. Fusion **42**, 443 (2000).
- [5] W.M. Tang *et al.*, Phys. Fluids B **5**, 2451 (1993).
- [6] W.M. Tang, Nucl. Fusion **18**, 1089 (1978).
- [7] Jiquan Li *et al.*, Phys. Plasmas **3**, 3337 (1996).
- [8] M.N. Rosenbluth *et al.*, Phys. Rev. Lett. **80**, 724 (1998).
- [9] R. Marchand *et al.*, Phys. Fluids **23**, 1164 (1980).
- [10] X.Q. Xu *et al.*, Phys. Fluids B **3**, 1807 (1991).
- [11] W.M. Tang *et al.*, Phys. Fluids **20**, 430 (1977).